Appl Biochem Biotechnol (2013) 169:773–785
DOI 10.1007/s12010-012-0014-0

In Silico and Experimental Characterization of Chimeric *Bacillus thermocatenulatus* Lipase with the Complete Conserved Pentapeptide of *Candida rugosa* Lipase

Mostafa Hosseini · Ali Asghar Karkhane · Bagher Yakhchali · Mehdi Shamsara · Saeed Aminzadeh · Dena Morshedi · Kamahldin Haghbeen · Ibrahim Torktaz · Esmat Karimi · Zahra Safari

Received: 16 September 2012 / Accepted: 3 December 2012 /
Published online: 29 December 2012

Abstract Lipases are one of the highest value commercial enzymes as they have broad applications in detergent, food, pharmaceutical, and dairy industries. To provide chimeric *Bacillus thermocatenulatus* lipase (BTL2), the completely conserved pentapeptide (^{112}Ala-His-Ser-Gln-Gly^{116}) was replaced with similar sequences (^{207}Gly-Glu-Ser-Ala-Gly^{211}) of *Candida rugosa* lipase (CLR) at the nucleophilic elbow region. For this purpose, three mutations including A112G, H113E, and Q115A were inserted in the conserved pentapeptide sequence of *btl2* gene. Based on the crystal structures of 2W22, the best structure of opened form of the chimeric lipases were garnered using the MODELLER v9.10 software. The native and chimeric lipases were docked to a set of ligands, and a trial version of Molegro Virtual Docker (MVD) software was used to obtain the energy values. Docking results confirmed chimeric lipase to be better than the native lipase. Following the in silico study, cloning experiments were conducted and expression of native and chimeric *btl2* gene in *Pichia pastoris* was performed. The native and chimeric lipases were purified, and the effect of these mutations on characteristics of chimeric lipase studied and then compared with those of native lipase. Chimeric lipase exhibited 1.6-fold higher activity than the native lipase at 55 °C. The highest percentage of both lipases activity was observed at 60 °C and pH of 8.0. The ion Ca^{2+} slightly inhibited the activity of both lipases, whereas the organic solvent enhanced the lipase stability of chimeric lipase as compared with the native lipase. According to the results, the presence of two glycine residues at the conserved pentapeptide region of this chimeric lipase (^{112}**Gly**-Glu-Ser-Ala-**Gly**^{116}) may increase the flexibility of the nucleophilic elbow region and affect the enzyme activity level.

Electronic supplementary material The online version of this article (doi:10.1007/s12010-012-0014-0) contains supplementary material, which is available to authorized users.

M. Hosseini · A. A. Karkhane (✉) · B. Yakhchali · M. Shamsara · S. Aminzadeh · D. Morshedi · K. Haghbeen · I. Torktaz · E. Karimi · Z. Safari
Department of Industrial and Environmental Biotechnology, National Institute of Genetic Engineering and Biotechnology (NIGEB), P.O. Box 14965/161, Tehran, Iran
e-mail: karkhane@nigeb.ac.ir

Keywords In silico · *Bacillus thermocatenulatus* · Conserved pentapeptide · Docking

Introduction

Lipases (triacylglycerol acylhydrolases, EC 3.1.1.3) belong to the class of α/β hydrolase superfamily that catalyzes the hydrolysis of emulsified long-chain triacylglycerol at the lipid–water interface [1]. Lipases have been used widely in industrial applications due to their ability to catalyze both hydrolysis and synthesis of long-chain acylglycerols reaction [2]. The catalytic triad of lipases is consisted of Ser, His, and Asp/(Glu) in which the catalytic Ser is located in a lipase-specific consensus sequence (Gly-X-Ser-X-Gly). In most *Bacillus* lipases, the first glycine is replaced by an alanine (Ala-X-Ser-X-Gly) [3–5]. Eggert et al. have investigated the role of this Ala residue by constructing LipB variant A76G of *Bacillus subtilis* lipase [6, 7]. This mutation showed a markedly reduced thermostability at pH11 but an increased stability at pH5–7 [6, 7].

Bacillus thermocatenulatus lipase (BTL2) is composed of a complete sequence of 417 residues including a 29-residue signal sequence that is cleaved to produce the mature 388-residue with molecular weight of about 43 kDa. Due to its high catalytic activity, thermal stability, stability in wide range of organic solvents, and the ability to hydrolyze a wide range of substrates, BTL2 is considered an attractive enzyme for biotechnological applications [8]. The BTL2 showed the highest activity toward tributyrin, although it has been observed to hydolyze triacylglycerols with C_4–C_{18} acyl groups. The active site of the BTL2 contains a catalytic triad consisting of serine 114, aspartic acid 318, and histidine 359. The nucleophilic Ser 114 is located in a γ-like turn, in a highly conserved Ala-His-Ser-Gln-Gly pentapeptide. This conserved pentapeptide which is located between the β5-strand and α-helix 4 is known as the nucleophile elbow [3]. The nucleophile elbow allows the nucleophilic Ser114 to have access to histidine (His357) on one site and substrate on the other site [9, 10].

Candida rugosa (formerly *Candida cylindracea*) lipase (CRL) is an important industrial enzyme that is widely used in biotechnological applications such as the production of fatty acids and the synthesis of various esters [11]. *C. rugosa* lipase (CRL) consists of 534 amino acids with an apparent MW of 60 kDa [12]. Since *C. rugosa* lipase (CRL) has been widely used in various industrial applications, we chose the conserved pentapeptide of CRLs (^{207}Gly-Glu-Ser-Ala-Gly^{211}) as a model to be replaced by the corresponding sequence of the *B. thermocatenulatus* lipase (^{112}Ala-His-Ser-Gln-Gly^{116}) [11].

All investigations in the conserved pentapeptide (Ala-X-Ser-X-Gly and Gly-X-Ser-X-Gly) of the lipases so far were carried out by replacing Ala with Gly [6, 7] and vice versa [13]. In the current study, we investigated for the first time the effect of replacing a complete conserved pentapeptide (^{112}Ala-His-Ser-Gln-Gly^{116}) of the BTL2 lipase with the correspondent sequence of *C. rugosa* lipase (PDB; 1CRL) (^{207}Gly-Glu-Ser-Ala-Gly^{211}) by making point mutations at the position of 112 (Ala to Gly), 113 (His to Glu), and 115 (Gln to Ala). The influence of mutations on lipase–substrate interaction, thermal activity, and stability was subsequently studied using computational and experimental methods.

Materials and Methods

Materials

The plasmid pYRK^{T}.BTL2 (previous work) was used for amplification of *btl2* gene and *Escherichia coli* strain TOP 10 (Invitrogen) as a host for molecular cloning of recombinant

pTZ57R/T (Fermentas) and pPICZαB (Invitrogen) plasmids harboring native and mutant *btl2* gene, respectively. *Pichia pastoris* GS115 (Invitrogen) was also used for heterologous protein expression. All media and protocols for *Pichia* are as described in the *Pichia* expression manual (Invitrogen). The ligand molecules that were used in this study include dibutyrin (C_4), tributyrin (C_4), tricaproin (C_6), and tricaprylin (C_8).

In Silico Studies

Homology Modeling and 3D-Structure Analysis

Amino acid sequence of the BTL2 lipase from the *B. thermocatenulatus* (accession no. CAA64621.1) was retrieved from the GenBank database (http://www.ncbi.nlm.nih.gov). BLASTP search [14] of a query (BTL2 sequence) was performed against Protein Data Bank (PDB). Homology modeling for the native and the chimeric lipases from the *B. thermocatenulatus* was performed by MODELLER v9.10 (http://www.salilab.org/modeller/) [15] using opened form of BTL2 lipase (2W22) downloaded from PDB server as template.

The MODELLER generated structure of the chimeric lipase was further analyzed by Ramachandran analysis generated by Procheck [16], Errat plot [17], Qmean server [18], ProSA-web [19], and RMSD value calculation [20]. Qmean is a parameter (between 0 and 1) for estimation of model reliability and ProSA displays quality score of predicted model in the context of all known protein structures. Furthermore, the structural similarity between native and chimeric lipases was checked by the RMSD value calculation using VMD software [20].

Molecular Docking Study

The molecular docking of native and chimeric lipase with a set of ligands (dibutyrin, tributyrin, tricaproin, and tricaprylin) was performed using the trial Molegro Virtual Docker 5.0 [21]. During docking, at first the molecules were prepared, and explicit hydrogens, charges, and flexible torsions were assigned if they were missing in the MVD program to both the protein (substrate) and ligands. Other docking parameters were set to the software's default values (Table 1).

Experimental Studies

Cloning of Chimeric *btl2* Gene

The plasmid pYRKT.BTL2 harboring the *btl2* gene (previous work) was used as a template for generating chimeric *btl2* gene using splicing by overlap extension method (SOE) as described previously [22]. The first PCR was carried out with E.F1 and E.R2 (5′-AGCTGCAGCATCCC CACGCGCCAATG-3′, *Pst* I site and 5′-GCGGGCCGTCTGTCCTCCAGCGCTTTCTCC GATGATATGGACGCGGCCG-3′) primers. The second PCR was performed using E.F3 and E.R4 (5′-CGGCCGCGTCCATATCATCGGAGAAAGCGCTGGAGGACAG ACGGCCCGC-3′ and 5′ TCTCTAGATCATTAAGGCCGCAAACTCGC-3′, *Xba* I site) primers. Then, PCR products (367 bp and 867 bp) were extracted and used for the third round of PCR using the primer pair, E.F1 and E.F4. Subsequently, the PCR product (1,185 bp) was cloned into pTZ57R/T leading to the formation of pKHT.E plasmid. To confirm the mutations

Table 1 Parameters used in the molecular docking studies

Scoring function	– Score: MolDock score
	– Grid resolution (Å): 0.30
Binding site	– Origin: user defined
	– Center: X=25.25, Y=−10.92, Z=−24.05
	– Radius: 11 Å
Search algorithm	– Algorithm: MolDock SE
	– Number of runs: 10
	– Constrain poses to cavity: yes
	– Energy minimization: yes
	– Optimized H-bonds: yes
Parameter settings	– Maximum iterations: 1,500
	– Maximum population size: 50
Pose generation	– Energy threshold: 100.0
	– Tries. Minimum: 10, Quick: 10, Maximum: 30
Simplex evolution	– Maximum steps: 300
	– Neighbor distance factor: 1.00
Return multiple poses for each run	– Maximum number of poses returned: 5
	– Enable energy threshold: no
	– Cluster similar poses. RMSD threshold: 1.00
	– Ignore similar poses (for multiple runs only). RMSD threshold: 1.00

in the *btl2* gene, the recombinant pKHT.E plasmid DNA was sequenced using universal M13 forward and reverses primers (Macrogen Inc., Seoul, South Korea). The pKHT.E plasmid was digested with *Pst* I and *Xba* I, and the resulting fragments (1,177 bp) were then ligated into the corresponding restriction sites of the pPICZαB to construct the pKH.picE plasmid. Finally, the *Sac* I linearized plasmid pKH.picE was introduced into the yeast *P. pastoris* GS115 by electroporation according to manufacturer's procedures. Subsequently, total genomic DNA from the yeast was prepared by boiling method and the integration of recombinant pKH.picE plasmid into the *P. pastoris* genome confirmed by PCR using AOX forward and reverse primers.

Expression and Purification

A single colony of recombinant *P. pastoris* was cultured in YPG medium (1 % yeast extract, 2 % peptone, and 1 % glycerol) at 28 °C (220 rpm) until the optical density of culture medium at 600 nm (OD_{600}) reached 4–6. The cells were harvested and transferred into 250 ml BMMH medium (1.34 % YNB, 4×10 5 % biotin, 0.5 % methanol, 0.4 % histidine, 100 mM potassium phosphate, pH 6.0) to produce a suspension with OD_{600} of 1. The expression of lipase was induced by methanol at 0.75 % at 24-h intervals for 96 h, and the lipase activity was assayed at 24-h intervals by using *p*-nitrophenyl palmitate (pNPP) as substrate [23].

The supernatant of the culture medium was separated by centrifugation (4,000 rpm, 10 min, 4 °C) and concentrated using a freeze-drying process. The concentrated supernatant was dialyzed against dialysis buffer (50 mM Tris–HCl, pH 4.5) and then loaded on a DE-52 cellulose column (Whatman, Maidstone, UK) equilibrated with dialysis buffer. All fractions were assayed for lipase activity and the fractions showing lipase activity were pooled and

concentrated as purified lipase. The purified lipases were dialyzed against dialysis buffer (10 mM Tris–HCl, pH 8.5) at 4 °C and store at −20 °C.

Substrate Specificity

Substrate specificity and chain length selectivity of lipases were determined in a pH-STAT using a variety of tributyrin (C4), tricaprin (C_6), tricaprylin (C_8), tricaprin (C_{10}), trilaurin (C_{12}), trimyristin (C_{14}), tripalmitin (C_{16}), and olive oil (C_{18}) as substrates. The assay was performed at pH 8.0 at 55 °C [22].

Effect of Temperature on Lipase Activity and Stability

The lipase activity was measured in a pH-STAT (Titrando 842; Metrohm, Switzerland) at pH 8.5 at 45, 50, 55, 60, and 65 °C using tricaprylin as substrate. Thermostability of the lipases was analyzed by measuring the residual lipase activity after incubating the enzymes for 15, 30, 45, and 60 min at 65 °C [22].

Effect of pH on Lipase Activity

The pH stability of the lipases was analyzed after 15-min incubation of lipases at pH range of 6.0 to 10.0. This assay was performed in a pH-STAT at 55 °C using tricaprylin as substrate [22].

Effect of Metal Ions, Organic Solvents, and Detergents on Lipase Activity

To determine the effect of metal ions on lipase activity, the lipases were incubated with metal ions including Ca^{2+}, K^{+}, Na^{+}, Mg^{2+}, and Mn^{2+} (1 mM) for 30 min. To study the effect of organic solvents on lipase activity, the lipases were incubated with acetone, *N*-heptane, *N*-hexane, methanol, and chloroform (30 %) for 60 min, and to investigate the effect of detergents on activity, the lipases were incubated with Tween 20, Tween 40, Tween 80, and SDS (1 %) for 75 min. Subsequently, the residual lipase activity was assayed in a pH-STAT at pH 8.0 at 55 °C using tricaprylin (C_8) as substrate [22].

Results and Discussion

Homology Modeling and Structure Validation

Homology modeling was performed to predict 3D structures (opened form) of the native and chimeric BTL2 lipases. The amino acid sequence of BTL2 retrieved from NCBI database (accession no. CAA64621.1) was used as a template in BLASTP [13] search against PDB to find suitable templates for homology modeling. Based on sequence identity between the query and the reference protein sequence, the PDB number of 2w22 with 99 % identity was identified for prediction of opened form of both lipases [24]. After the alignment between templates and query sequence was performed, the best structure model of native and chimeric lipases was garnered using MODELLER v9.10 (Fig. 1) [15].

The MODELLER-generated structure was further assessed by Ramachandran plot generated by Procheck [16], Errat plot [17], Qmean server [18], ProSA-web [19], and root-mean-square deviation (RMSD) [20]. ProSA and QMEAN scores for the chimeric

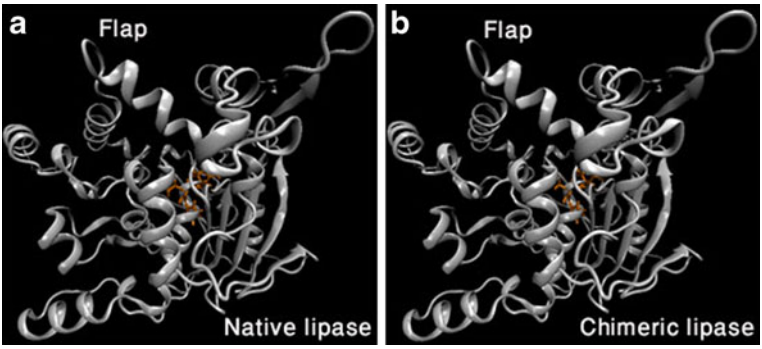

Fig. 1 Optimized 3D structure of the opened form of both lipases generated by MODELLER v9.10 using 2W22 as the template. **a** 3D structure of the native lipase. **b** 3D structure of the chimeric lipase. The protein structures are shown as new cartoon representation. Visualization was performed using VMD software [20]

lipase were found to be −8.31 and 0.810 (Z-score = 0.47), respectively. Ramachandran plot of the chimeric lipase showed that 94.2 % of the amino acid residues were present in the most favored region, 5.5 % in additional allowed region, and 0.3 % in the generously allowed region (Fig. 2). From the above results, it is understood that more than 90 % of amino acid residues are in the most favored region and the modeled chimeric lipase has a good quality. Further analysis of the Ramachandran dihedral angles (Φ, ψ) of the residues located at conserved pentapeptide sequence of the native and chimeric lipases reveals that the angles of both lipases are very close to each other (Table 2).

In addition, the quality of structure was further analyzed using ERRAT [17]. The overall quality factor was around 94.474, which is very much acceptable, and suggested that the model is reliable (Fig. 3).

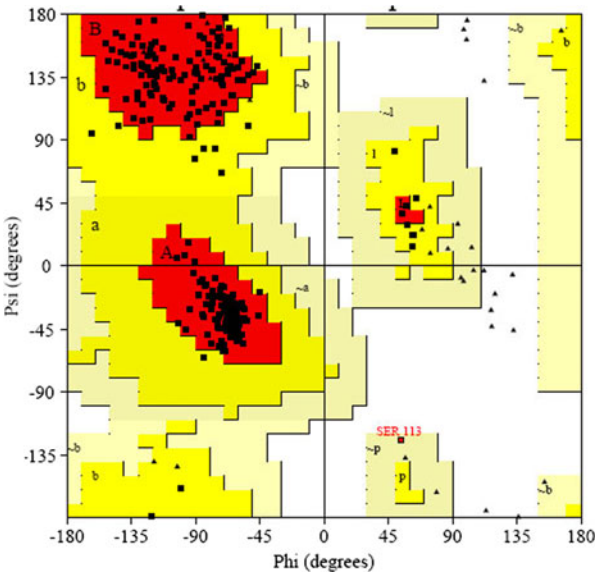

Fig. 2 Ramachandran plot validation of chimeric lipase generated by Procheck. Glycine residues are shown with *triangle* and all other residues are shown with a *square*

Table 2 Parameters of the conserved pentapeptide sequences

	Native BTL2		Chimeric BTL2	
Residue	Φ	ψ	φ	ψ
^{112}Ala/^{112}Gly	−125.30	152.80	−126.30	153.12
^{113}His/^{113}Glu	−118.69	134.47	−117.56	135.75
^{114}Ser	55.28	−125.61	53.74	−124.33
^{115}Gln/^{115}Ala	−55.93	−29.39	−55.66	−30.81
^{116}Gly	−55.29	−30.06	−55.15	−29.69

^{112}Ala/^{112}Gly alanine in the conserved pentapeptide of the native lipase corresponds to the glycine in the conserved pentapeptide of the chimeric lipase, *^{113}His/^{113}Glu* histidine in the conserved pentapeptide of the native lipase corresponds to the glutamic acid of the chimeric lipase, *^{115}Gln/^{115}Ala* glutamine in the conserved pentapeptide of the native lipase corresponds to the alanine of the chimeric lipase

Furthermore, the RMSD of Cα atoms between template and model (chimeric lipase) was calculated after superimposing both lipases (388 residues). An RMSD of 0.22 Å was found between the model and the template structures [20]. This result indicates that the structures of the chimeric and template are similar and the homology model is reliable (Fig. 4).

The distance between side chains of catalytic Ser114 and His 359 is an important factor contributing to lipase activity which was found to be 3.04 Å and 3.19 Å for native and chimeric lipases, respectively (Fig. 5). For the chimeric lipase, the distance increases by 0.15 Å. However, these mutations do not affect the conformation of the conserved pentapeptide residues at the nucleophilic elbow site since the distance between the side chain of catalytic Ser114 and His359 in both lipases remains the same.

Docking Study

Docking study was performed using trial version of Molegro Virtual Docker [21] using a set of ligands including dibutyrin, tributyrin, tricaproin, and tricaprylin generated by PubChem compound database [25]. MolDock scores for the chimeric lipase revealed a slight increase in ligand–protein binding affinity (Table 3).

In silico analysis demonstrated that replacing the complete conserved pentapeptide of *Bacillus* lipase with the similar sequence in *C. rugosa* lipase can improve the activity level of BTL2 lipase. Moreover, to confirm the in silico analysis results,

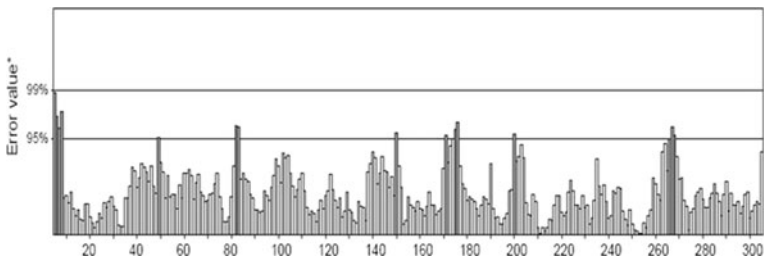

Fig. 3 Errat plot for the chimeric lipase model. *Black bars* show the misfolded region, *gray bars* demonstrate the error region between 95 % and 99 %, and *white bars* indicate the region having less error rate for protein folding

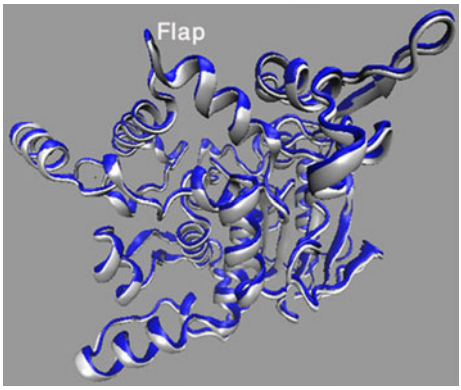

Fig. 4 Superposition of template (*light ribbon*) with the predicted model of chimeric lipase (*dark ribbon*). The picture has been taken with VMD [20]

experimental studies were performed by replacing the conserved pentapeptide using site-directed mutagenesis.

Experimental Data

Mutants and Expression

Since *C. rugosa* lipase (CRL) has been widely used in various industrial applications, we intended to choose the conserved pentapeptide of CRL (^{207}Gly-Glu-Ser-Ala-Gly^{211}) as a model to be replaced by the corresponding sequence of the *B. thermocatenulatus* lipase (^{112}Ala-His-Ser-Gln-Gly^{116}) [12]. For this purpose, three mutations including A112G, H113D, and Q115A were exerted in the conserved pentapeptide region of the *B. thermocatenulatus* lipase using splicing by overlap PCR (SOE-PCR). The native and chimeric lipase genes were cloned in a cloning vector (pTZ57R/T). The presence of mutations in the gene was confirmed by DNA sequencing and then both lipase genes were sub-cloned in an expression vector (pPICZαB) downstream of the α-factor signal sequence. The expression vectors were linearized and transformed into yeast *P. pastoris* GS115 by electroporation and expressed according to manufacturer's procedures. The lipases were purified (Fig. 6a) and

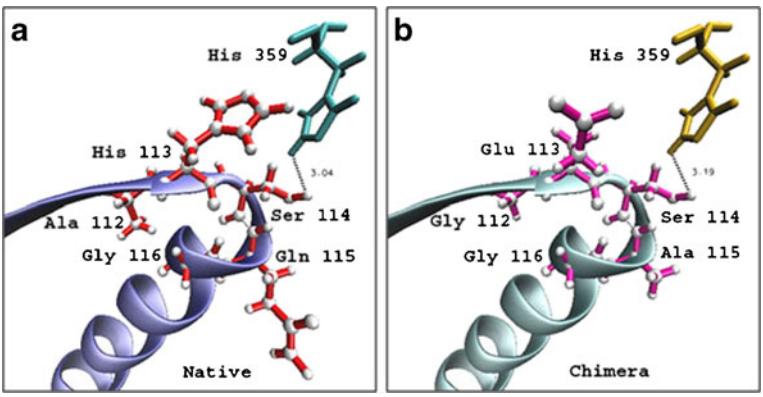

Fig. 5 Interatomic distances between side chains of catalytic serine and histidine residues at the active site of **a** native and **b** chimeric lipases

Table 3 The docking results of a set of substrates to the native and chimeric BTL2

MolDock score (kcal/mol) (X=25.25, Y=−10.92, Z=−24.05, R=11)		
Substrate	Native BTL2	Chimeric BTL2
Dibutyrin	−89.851	−100.65
Tributyrin	−93.981	−108.55
Tricaproin	−71.538	−103.55
Tricaprylin	−31.046	−97.745

checked with western blot (Fig. 6b) as mentioned above and they were used to study the effect of conserved pentapeptide sequence of CRL lipase on BTL2 lipase specifications.

Chimeric Lipase Characterizations

Lipase Activity and Substrate Specificity

The activity and substrate specificity of chimeric lipase was compared to the native lipase in pH-STAT at 55 °C and pH8.5 with a broad range of lipase substrates from C_4 to C_{18}. The chimeric lipase showed higher specific activities versus native lipase against all substrates except for trimyristin (1,390 U/mg) and tripalmitin (684 U/mg) with maximal activity toward tributyrin (11,823 U/mg) and tricaprylin (7,914 U/mg) substrates (Fig. 7). These observations are in accordance with a previous study reporting that the maximum activity and specificity of *B. thermocatenulatus* lipase is toward small triglyceride substrates such as tributyrin [23].

Thermal Activity and Stability

The effect of temperature on native and chimeric lipases is shown in Fig. 8a. The results showed that the highest percentage of activity of both lipases were at 60 °C, which is the

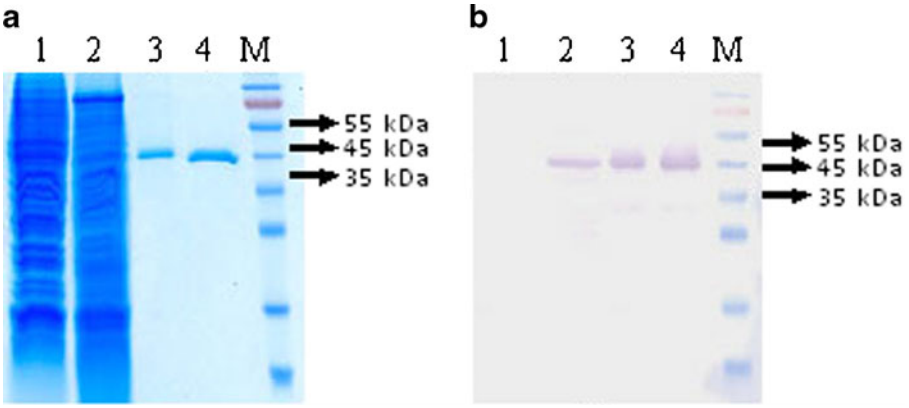

Fig. 6 SDS–PAGE (**a**) and Western blot (**b**) analysis of purified native and chimeric lipases. *Lanes 1–2* total recombinant yeast proteins before and after methanol induction, *3–4* purified native and chimeric recombinant lipases, *M* protein size marker

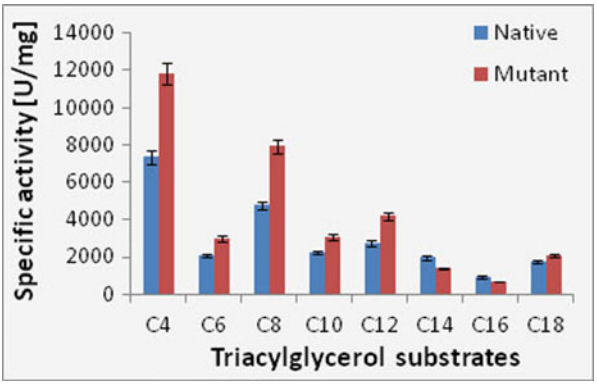

Fig. 7 The activity and substrate specificity of purified native (*black bars*) and chimeric (*gray bars*) lipase toward substrates with different acyl chain lengths from C4 to C18. The assay was performed in a pH-STAT (at 55 °C) and pH 8.5

optimal reaction temperature. For both lipases, the relative activity was found to be increased as the temperature increased from 45 °C to 60 °C. At temperatures above 60 °C, the relative activity was drastically reduced and further decrease was observed at a temperature of 65 °C (Fig. 8a). The result shows that for both lipases, decrease in activity occurs at higher temperatures. Figure 8b shows the thermal stability of chimeric lipase compared to the native lipase. However, for both lipases the thermal stability decreased with increase in incubation time from 0 to 60 min at 65 °C. It may be due to destruction of protein structure by heat, which caused protein unfolding and led to loss of lipase activity [26]. Eggert et al. studied the role of Ala residue in the conserved pentapeptide (Ala-X-Ser-X-Gly) of the *B. subtilis* lipase by constructing LipB variant A76G which showed a notably reduced thermostability in contrast to the increased stability of the lipase [6, 7]. On the contrary, Jeong et al. [13] indicated that the replacement of Gly by Ala in the conserved pentapeptide sequence could lead to an enhanced thermostability in *Bacillus* lipases because the side chain of the Ala residue stabilizes the loop conformation by tight packing. However, Gly is a unique residue among the other amino acids with smaller side chain and it cannot stabilize the loop conformation as Ala does. Therefore, changing Ala to Gly (A112G) causes a decrease in thermal stability of lipase. To evaluate the change in protein stability after having mutations, the thermodynamic stability ($\Delta\Delta G$) using flexible and fixed backbone method was calculated by Eris server [27], which was found to be 5.08 kcal/mol and 0.83 kcal/mol, respectively. The results showed that the chimeric lipase is slightly unstable compared to the native lipase.

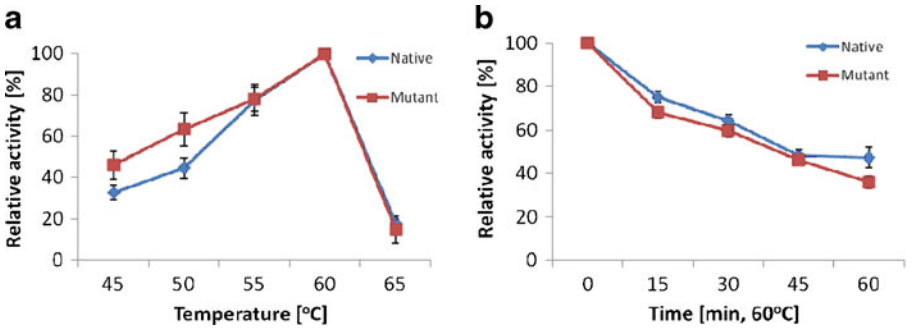

Fig. 8 Thermal activity and stability of lipase. **a** Effect of different temperatures on the activity of native and chimeric lipases. **b** Effect of temperature on the stability of native and chimeric lipases after incubation at 65 °C in various time intervals

Effect of pH, Detergents, Organic Solvent, and Metal Ions on Lipase Activity

The effect of pH on both lipases is shown in Fig. 9a. A 100 % relative activity was equal to the specific activities at pH of 8.0 that were 7,543 U/mg and 4,213 U/mg for chimeric and native lipases, respectively. The results revealed that the highest percentage of activity for both lipases were at pH of 8.0 which was in agreement with the results obtained by Schmidt-Dannert et al. [28]. At pH values above 8.0, for both lipases, particularly for the chimeric lipase, the relative activity was decreased with increase in pH up to 10.0 [28]. It is observed that the chimeric lipase was slightly sensitive to pH values above 8.0 (alkaline conditions), owing to the mutation at its conserved pentapeptide region (Fig. 9a).

The effect of detergents on lipase activity is shown in Fig. 9b. In general, most detergents stimulated the activation of both lipases. The results showed that Tween 20, Tween 40, Tween 80, and Triton X-100 enhanced and SDS extremely decreased the catalytic activities of both lipases. It was found that SDS has the highest impact on both lipases by decreasing the activity of both chimeric and native lipases compared to the control by approximately 80.5 % and 52 %, respectively. The results showed that both lipases were highly sensitive to inhibition by SDS. Moreover, non-ionic detergents facilitate the breakdown of lipase aggregates and cause an elevation in lipase activity, whereas SDS (1 %) cause conformational changes and/or disrupt substrate binding and leads to a decrease in lipase activity [29].

Figure 9c shows the effect of organic solvents on activity of both lipases. Increase in activity was observed for chimeric lipase in presence of organic solvents. Those results showed that the chimeric lipase was stable in the organic solvents. Acetone, methanol, hexane, heptane, and chloroform enhanced the lipase stability of chimeric lipase as compared with the native lipase, whereas these did not significantly affect the enzyme activity of native lipase. The influence of organic solvents and also detergents in producing open

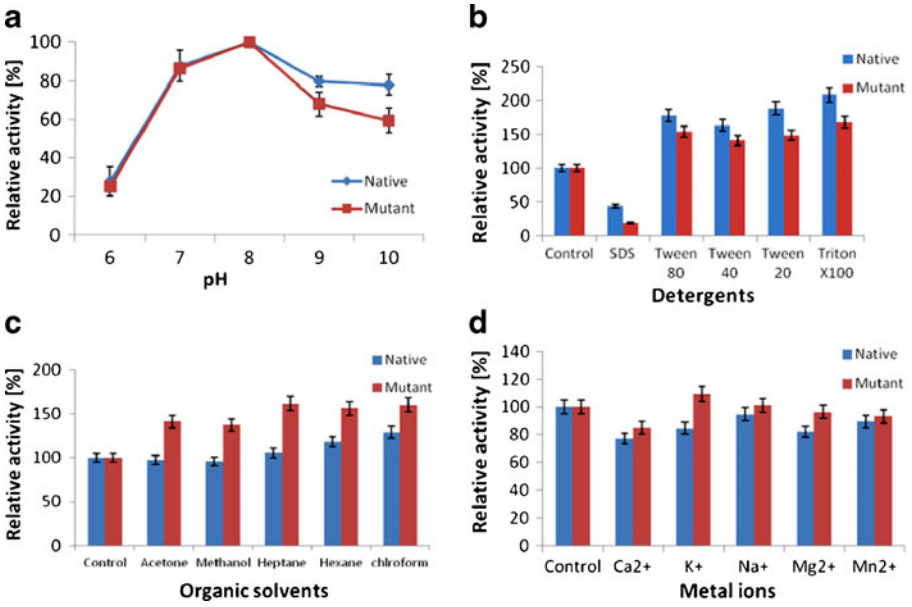

Fig. 9 Summary of the relative activity profiles of both lipases in different **a** pH values, **b** detergents, **c** organic solvents, and **d** metal ions

conformations might suggest that the dielectric constant of the surrounding solvent is in favor of lid movement [30].

Figure 9d shows the effect of metal ions on activity of both lipases. The results showed that Ca^{2+} slightly inhibited the activity of both lipases. However, adding 1 % of Ca^{2+} to the assay mixture revealed a 15 % and 23 % decrease in the activity of chimeric and native lipases, respectively. The ion K^{+} slightly stimulated the lipase activity of chimeric lipase and Na^{+}, Mg^{2+}, and Mn^{2+} did not significantly affect the enzyme activity. Similar results have also been reported by Rahman et al. [31] which confirm the results of this study indicating that metal ions such as Ca^{2+} stimulate lipase activity after 15 min of incubation, whereas prolonged incubation (30 min) leads to decreased enzyme activity. Lipases show variable stability towards various metal ions due to the ions often playing a structural rather than a catalytic role [31].

Conclusion

Docking is a powerful technique for studying the effect of mutations on protein–ligand interaction. In this study, we have carried out the docking analysis before and after mutating the lipase to find minimum binding energy between lipase and substrate. Docking results confirmed that after lipase mutation, the binding energy between chimeric lipase and substrates becomes lower than that between native lipase and substrates (Table 2). Experimental data confirmed the results of bioinformatics studies stating that the alterations improved native lipase activity. The results showed that replacement of complete conserved pentapeptide of the *Bacillus* lipase with the similar sequence in *C. rugosa* lipase can improve some properties of native lipase such as activity. Glycine is one of the conserved residues in conserved pentapeptide of both *Bacillus* and *Candida* species. Also, it was previously reported that glycine has a role in protein flexibility because it lacks a side chain and Cβ. The absence of the Cβ atom allows the glycine Ramachandran plot to run over the borders at −180° and 180° [32]. In a nutshell, presence of two glycine residues at the conserved pentapeptide sequence of chimeric lipase (^{112}**Gly**-Glu-Ser-Ala-**Gly**^{116}) may lead to an increase in flexibility of the nucleophilic elbow region and affect the enzyme activity level. In a study performed by Tsou et al. [33, 34], it was observed that the flexibility of the enzyme active site affects enzyme activity, thus the active site of the chimeric enzyme may be conformationally more flexible than the native one. Therefore, an increase in active site flexibility at the nucleophilic elbow region of the enzyme facilitates the access of catalytic Ser114 to the catalytic His359 on one site and substrate from another site that would lead to a better hydrolysis activity. Altogether, we can conclude that for industrial applications this modified lipase seems to work better than the native lipase especially at temperatures around 60 °C.

Acknowledgment This study has been supported by the Iran National Science Foundation (INSF), research project no. 88002118, for which the authors are very grateful.

References

1. Widmann, M., Juhl, P. B., & Pleiss, J. (2010). *BMC Genomics, 11*, 123.
2. Jaeger, K. E., & Reetz, M. T. (1998). *Trends in Biotechnology, 16*, 396–403.
3. Schrag, J. D., & Cygler, M. (1997). *Methods in Enzymology, 284*, 85–107.
4. Messaoudi, A., Belguith, H., & Ben Hamida, J. (1998). *Biochemistry Journal, 322*, 75–80.
5. Kim, H. K., Park, S. Y., Lee, J. K., & Oh, T. K. (1998). *Bioscience, Biotechnology, and Biochemistry, 62*, 66–71.

6. Eggert, T., Pouderoyen, G. V., Dijkstra, B. W., & Jaeger, K. E. (2001). *FEBS Letters, 502*, 89–92.
7. Eggert, T., van Pouderoyen, G., Pencreac'h, G., Douchet, I., Verger, R., Bauke, W., Dijkstra, B. W., & Jaeger, K.-E. (2002). *Colloids and Surfaces. B, Biointerfaces, 26*, 37–46.
8. Schlieben, N. H., Niefind, K., & Schomburg, D. (2004). *Protein Expression and Purification, 34*, 103–110.
9. Jaeger, K. E., Dijkstra, B. W., & Hertz, M. T. (1999). *Annual Review of Microbiology, 53*, 315–351.
10. Ollis, D. L., Shea, E., Cygler, M., Dijkstra, B., Frolow, F., Franken, S. M., Harel, M., Remington, S. J., Silman, I., Schrag, J., Sussman, J. L., Verschueren, K. H. G., & Goldman, A. (1992). *Protein Engineering, 5*, 197–211.
11. Lee, L. C., Chen, Y. T., Yen, C. C., Chiang, T. C., Tang, S. J., Lee, G. C., & Shaw, J. F. (2007). *Journal of Agricultural and Food Chemistry, 55*, 5103–5108.
12. Lotti, M., Tramontano, A., Longhi, S., Fusetti, F., Brocca, S., Pizzi, E., & Alberghina, L. (1994). *Protein Engineering, 7*, 531–535.
13. Jeong, S. T., Kim, H. K., Kim, S. J., & Chi, S. W. (2002). *Journal of Biological Chemistry, 277*, 17041–17047.
14. Altschul, S. F., Madden, T. L., Schäffer, A. A., Zheng, J., Zhang, Z., Miller, W., & Lipman, D. J. (1997). *Nucleic Acids Research, 25*, 3389–3402.
15. Eswar, N., Marti-Renom, M.A., Webb, B., Madhusudhan, M., Eramian, S.D., Shen, M., Pieper, U., & Sali, A. (2006). *Current Protocols in Bioinformatics*. New York: Wiley, Supplement 15, pp. 5.6.1–5.6.30.
16. Laskowski, R. A., MacArthur, M. W., Moss, D. S., & Thornton, J. M. (1993). *Journal of Applied Crystallography, 26*, 283–291.
17. Colovos, C., & Yeates, T. O. (1993). *Protein Science, 2*, 1511–1519.
18. Benkert, P., Tosatto, S. C. E., & Schomburg, D. (2008). *Proteins: Structure, Function, and Bioinformatics, 71*, 261–277.
19. Wiederstein, M., & Sippl, M. J. (2007). *Nucleic Acids Research, 35*, W407–W410.
20. Humphrey, W., Dalke, A., & Schulten, K. (1996). *Journal of Molecular Graphics, 14*, 33–38.
21. Thomsen, R., & Christensen, M. H. (2006). *Journal of Medicinal Chemistry, 49*, 3315–3321.
22. Karkhane, A. A., Yakhchali, B., Rastgar Jazii, F., & Bambai, B. (2009). *Journal of Molecular Catalysis B: Enzymatic, 61*, 162–167.
23. Quyen, D. T., Schmidt-Dannert, C., & Schmid, R. D. (2003). *Protein Expression and Purification, 28*, 102–111.
24. Carrasco-Lopez, C., Godoy, C., De Las Rivas, B., Fernandez-Lorente, G., Palomo, J. M., Guisan, J. M., Fernandez-Lafuente, R., Martinez-Ripoll, M., & Hermoso, J. A. (2009). *Journal of Biological Chemistry, 284*, 4365–4372.
25. Bolton, E., Wang, Y., Thiessen, P. A., & Bryant, S. H. (2008). *Chapter 12 in Annual Reports in Computational Chemistry, Volume 4*. Washington: American Chemical Society.
26. Abdul Rahman, M. B., Md Tajudin, S., Hussein, M. Z., Abdul Rahman, R. N. Z., Salleh, A. B., & Basri, M. (2005). *Applied Clay Science, 29*, 111–116.
27. Yin, S., Ding, F., & Dokholyan, N. V. (2007). *Nature Methods, 4*, 466–467.
28. Schmidt-Dannert, C., Rua, M. L., Atomi, H., & Schmid, R. D. (1996). *Biochimica et Biophysica Acta, 1301*, 105–114.
29. Salameh, M. A., & Wiegel, J. (2010). *The Open Biochemistry Journal, 4*, 22–28.
30. Joseph, D., Yunge, L., Miroslaw, C., Dietmar, L., Tanja, B., Hans-Juergen, H., Rolf, S., et al. (1997). *Structure, 5*, 187–202.
31. Rahman, R. N. Z. A., Baharum, S. N., Basri, M., & Salleh, A. B. (2005). *Analytical Biochemistry, 341*, 267–274.
32. Yan, B. X., & Sun, Y. Q. (1997). *Journal of Biological Chemistry, 272*, 3190–3194.
33. Tsou, C. L. (1986). *Trends in Biochemical Sciences, 111*, 427–429.
34. Tsou, C. L. (1993). *Science, 262*, 380–381.